Leptin Receptor$^+$ cells create a perisinusoidal niche for thrombopoiesis in the bone marrow by synthesizing CXCL14

Yuanyuan Xue[1], Ruixuan Zhang[1], Amanda Reyes[1], Maowu Luo[2], Salma Merchant[1], Trevor Tippetts[1], Gerik Grabowski[1], Tai Ngo[3], Yanan Zhang[4], Zhiguo Shang[3], Nisi Jiang[1], Elise Jeffery[1], Yafeng Li[1], Tao Wei[1], Wen Gu[1], Liming Du[1], Ralph J. DeBerardinis[1,5,6], Kevin M. Dean[3], Thomas P. Mathews[1], Daniel Lucas[4], Zhiyu Zhao[1], Sean J. Morrison[1,5]

[1] Children's Research Institute and the Department of Pediatrics, University of Texas Southwestern Medical Center, Dallas, TX, USA.

[2] Department of Pathology, University of Texas Southwestern Medical Center, Dallas, TX, USA

[3] Lyda Hill Department of Bioinformatics, University of Texas Southwestern Medical Center, Dallas, TX, USA

[4] Division of Experimental Hematology and Cancer Biology, Cincinnati Children's Medical Center, Cincinnati, OH, USA

[5] Howard Hughes Medical Institute, UT Southwestern Medical Center, Dallas, TX, USA

[6] The Eugene McDermott Center for Human Growth and Development, UT Southwestern Medical Center, Dallas, TX, USA

Corresponding author: Sean J. Morrison, sean.morrison@utsouthwestern.edu, (214)648-2352

Short title: LepR$^+$ cells regulate thrombopoiesis via CXCL14

Word count for text: 3983

Word count for abstract: 200

Figures: 6

Tables: 0

References: 80

Scientific category: Platelets and thrombopoiesis

Data sharing statement: For original data, contact Sean.Morrison@UTSouthwestern.edu

Data and code availability

All data reported in this paper will be shared by the lead contact upon reasonable request. The RNA sequencing data generated in this paper have been deposited at the Sequence Read Archive BioProject ID PRJNA1225166. Source code related to the analysis of single-cell RNA sequencing, bulk RNA sequencing, and lipidomics data can be found at https://git.biohpc.swmed.edu/CRI/morrison-lab/scRNASeq, https://git.biohpc.swmed.edu/CRI/morrison-lab/RNASeq, and https://git.biohpc.swmed.edu/CRI/ODA, respectively. Any additional information required to reanalyze the data reported in this paper is available from the lead contact upon request.

Materials availability

A material transfer agreement is required to obtain *Cxcl14*^{flox} or *Cxcl14*^{dsRed} mice in accordance with the regulations of the University of Texas Southwestern Medical Center.

Key points

- Leptin Receptor^{+} stromal cells regulate terminal differentiation in megakaryocytes in addition to maintaining stem and progenitor cells
- CXCL14 from Leptin Receptor^{+} cells promotes the formation of platelets by remodeling lipid metabolism in megakaryocytes in the bone marrow

Abstract

Leptin Receptor-expressing (LepR$^+$) stromal cells in the bone marrow are a critical source of growth factors for the maintenance of hematopoietic stem cells (HSCs) and most restricted hematopoietic progenitors. An important unresolved question is whether they also regulate terminal differentiation in some hematopoietic cells. We found that LepR$^+$ cells promote thrombopoiesis by synthesizing the chemokine CXCL14, which is expressed in the bone marrow by a subset of LepR$^+$ cells. *Cxcl14*-expressing LepR$^+$ cells extend fine processes that wrap around perisinusoidal megakaryocytes. Deletion of *Cxcl14* from LepR$^+$ cells did not significantly alter HSC function or most aspects of bone marrow hematopoiesis, including megakaryocyte generation; however, it significantly reduced the numbers of proplatelet-forming megakaryocytes in the bone marrow and platelets in the blood. CXCL14 promoted platelet formation by remodeling lipid metabolism in megakaryocytes, increasing fatty acid transporter expression and enabling megakaryocytes to take up more polyunsaturated fatty acids from circulation. A high fat diet rescued the formation of proplatelet-forming megakaryocytes and platelets in *Lepr-cre; Cxcl14* $^{fl/fl}$ mice. CXCL14 protein was sufficient to promote platelet formation by megakaryocytes in vitro and in vivo. LepR$^+$ cells thus create a perisinusoidal niche for thrombopoiesis by producing CXCL14, which regulates lipid metabolism and terminal differentiation in megakaryocytes.

INTRODUCTION

Leptin Receptor-expressing (LepR$^+$) stromal cells promote the maintenance of hematopoietic stem cells (HSCs) and most restricted hematopoietic progenitors in the bone marrow by producing Stem cell factor (SCF)[1-3], CXCL12[4,5], Pleiotrophin[6], Interleukin 7 (IL7)[7], and Colony stimulating factor 1 (CSF1)[8-10]. LepR$^+$ cells have also been described as CXCL12-abundant reticular (CAR) cells[11,12]. Some LepR$^+$ cells are perisinusoidal, where they create niches for HSCs, erythroid progenitors, and other restricted hematopoietic progenitors[1,2,4,13-15]. Other LepR$^+$ cells are peri-arteriolar, where they create niches for lymphoid progenitors[16]. LepR$^+$ cells also promote vascular regeneration by producing Angiopoietin-1[17] and VEGF-C[18] as well as peripheral nerve maintenance in bone marrow by producing nerve growth factor[19]. However, it is unknown whether LepR$^+$ cells regulate terminal differentiation in any hematopoietic cells.

Platelets regulate hemostasis, inflammation, and tissue repair by enabling blood clotting[20]. Platelets are produced in the bone marrow by megakaryocytes[21,22], which localize to sinusoidal blood vessels[23,24] and release platelets into circulation[25]. A number of cytokines promote the formation of megakaryocytes in the bone marrow including thrombopoietin[26-28], SCF[29-31], leukemia inhibitory factor[32], fibroblast growth factor 4[33,34], IL-3, IL-6 and IL-11[29,35-38]. Thrombopoietin is produced by hepatocytes in the liver[39] and SCF is produced by LepR$^+$ cells in the bone marrow[1] but the cellular sources of other factors are uncertain.

Several other cytokines and chemokines promote the maturation of megakaryocytes into proplatelet-forming megakaryocytes or the generation of platelets including Insulin growth factor 1[40], IL-1a[41], chemokine ligand 5[42], and Interferon alpha (IFNα)[43]. IFNα is produced by plasmacytoid dendritic cells in the bone marrow[43] but to our knowledge the cellular sources of other cytokines and chemokines are uncertain.

CXCL14 is a chemokine that is expressed in multiple tissues[44], including in bone marrow stromal cells[45]. The receptor for CXCL14 is uncertain: CXCR4, which is widely expressed by hematopoietic cells, can serve as a receptor for CXCL14[46,47] but other receptors have been

suggested as well[48-52]. CXCL14 promotes immune cell migration to sites of inflammation[53,54] as well as platelet migration and thrombus consolidation[47]. However, CXCL14 has not been shown to play any role in the regulation of hematopoiesis or thrombopoiesis in the bone marrow.

METHODS

Mice

All mice were maintained on a C57BL/6 background. *Scf*^{GFP} (*Kitl*$^{tm1.1Sjm}$; a GFP knockin allele that reports *Scf* expression) was generated in our laboratory. *Lepr*^{cre} (B6.129(Cg)-Lepr$^{tm2(cre)Rck}$; a Cre allele expressed by *Lepr*$^{+}$ cells)[55] was obtained from Jackson Laboratory. *Prx1-cre* (B6.Cg-Tg(Prrx1-cre)1Cjt; a Cre allele expressed by limb mesenchymal cells)[56]. *Cxcl14*^{dsRed} and *Cxcl14*^{flox} mice were generated in this study. Male and female mice were used in most experiments. C57BL/Ka-Thy-1.1/ C57BL/Ka-Thy-1.2 (CD45.2/CD45.1) mice or C57BL/Ka-Thy-1.2 (CD45.1) mice were used as recipients or as a source of competitor bone marrow cells in transplantation experiments. Recipient mice were given Baytril (0.1 mg/ml in the drinking water) for 1 week prior to, and one month after, irradiation.

Mice were housed in the Animal Resource Center at UT Southwestern in a specific-pathogen-free facility under a 12 h:12 h light:dark cycle with a temperature of 18–24 °C and humidity of 35–60%. For experiments with high-fat diets, 4-5 month-old control and *Lepr-cre; Cxcl14*$^{fl/fl}$ mice were placed on the following diets: normal chow (Research Diets, D12450Ji), HFD1 diet (Research Diets, D22050405i), HFD2 diet (Research Diets, D12492i). All procedures were approved by the UT Southwestern Institutional Animal Care and Use Committee.

Measuring fatty acid uptake in vivo using $^{13}C_{18}$-linoleic acid

Jugular catheters were implanted in *Lepr-cre; Cxcl14*$^{fl/fl}$ and control mice. After a week of recovery, the mice were fasted for 4 hours, infused intravenously with $^{13}C_{18}$-linoleic acid conjugated to BSA for 24 hours, then blood and bone marrow were collected. CD42d^{+}

megakaryocytes were isolated from bone marrow using paramagnetic beads, then lipids were extracted and analyzed by LC/MS/MS[57]. We calculated the theoretical mass of isotopically labeled lipid species[58] then used these values to derive a library of isotopically labeled lipid species that included phospholipids, triglycerides, and free fatty acids. Lipidomic data were searched against this library with 5 ppm mass accuracy. Peaks that appeared to be isotopically labeled lipids were confirmed through MS/MS analysis. All data was corrected for naturally abundant isotopes and the fractional enrichments and pool sizes of each lipid were quantified.

Recombinant mouse CXCL14 treatment

Recombinant mouse CXCL14 (R&D, Catalog #: 730-XC) was intravenously injected into mice at a dose of 20 µg/kg body weight in a volume of 150 µl per mouse. The equivalent volume of sterile PBS was injected into control mice. The mice were analyzed 16 hours after injection.

Additional methods can be found in Supplementary Materials.

RESULTS

***Cxcl14* is mainly expressed by LepR$^+$ cells in the bone marrow**

To assess the *Cxcl14* expression pattern in the bone marrow, we reanalyzed published single cell RNA sequencing data from enzymatically dissociated bone marrow cells[59]. *Cxcl14* was expressed by LepR$^+$ cells but rarely by osteoblasts, chondrocytes, fibroblasts, endothelial cells, pericytes, or Schwann cells (Figure 1A). Quantitative reverse transcription PCR (qRT-PCR) confirmed *Cxcl14* was expressed by LepR$^+$CD45$^-$Ter119$^-$CD31$^-$ stromal cells but not by endothelial cells, HSCs or WBM cells (Figure 1B). *Cxcl14* was expressed by both *Osteolectin* negative *Lepr*$^+$ cells, which are perisinusoidal[1], and *Osteolectin*$^+$*Lepr*$^+$ cells, which are peri-arteriolar[16] (Figure 1A).

We generated a *Cxcl14*-dsRed (*Cxcl14* ^{dsRed}) knock-in reporter allele (Supplemental Figure 1A-C). Confocal imaging of femurs from adult *Cxcl14* $^{dsRed/+}$*; Scf* $^{GFP/+}$ mice showed *Cxcl14*

^{dsRed} expression by perisinusoidal and peri-arteriolar stromal cells (Figure 1C-E; Supplemental Figure 1C). The *Cxcl14* ^{dsRed}-expressing perisinusoidal stromal cells were *Scf*-GFP^{+} (Figure 1D and 1H) and LepR^{+} (Figure 1E).

Flow cytometric analysis of enzymatically dissociated bone marrow cells from adult *Cxcl14* $^{dsRed/+}$*; Scf* $^{GFP/+}$ mice showed that *Cxcl14* ^{dsRed} was expressed by 0.19±0.045% of bone marrow cells, 91±0.85% of which were LepR^{+} (Figure 1F). Furthermore, 89±1.5% of LepR^{+} cells were *Cxcl14* ^{dsRed} positive (Figure 1G). We rarely detected *Cxcl14* ^{dsRed} expression by endothelial cells (Figure 1I), hematopoietic cells in the bone marrow, including megakarocytes (Figure 1J; Supplemental Figure 1D), or platelets in the blood (Supplemental Figure 1E). The flow cytometry gates used to sort LepR^{+} cells and endothelial cells are in Figure 1G-I and the gates for hematopoietic cells are in Supplemental Figure 1F-I. Consistent with these data, reanalysis of published single cell RNA sequencing data[59,60] showed LepR^{+} cells expressed the highest levels of *Cxcl14* in the bone marrow at all ages, including postnatal day 4 (P4), P14 (Supplemental Figure 2A) and 2, 12, and 24 months of age (Supplemental Figure 2B). LepR^{+} cells thus appear to be the major source of *Cxcl14* in the bone marrow throughout life.

CXCL14 is required for thrombopoiesis but not megakaryopoiesis

To test if CXCL14 regulates hematopoiesis, we generated mice with a floxed *Cxcl14* allele by inserting loxp sites on either side of exon 2 (Supplemental Figure 3A-B). Cre mediated recombination would be predicted to cause a frameshift, yielding a strong loss of CXCL14 function. *Lepr-cre; Cxcl14* $^{fl/fl}$ mice were born in expected numbers and did not significantly differ from littermate controls in terms of gross appearance (Supplemental Figure 3C) or body mass (Supplemental Figure 3D). LepR^{+} cells had substantially lower levels of *Cxcl14* transcripts in 4 month-old *Lepr-cre; Cxcl14* $^{fl/fl}$ mice as compared to littermate controls (approximately 30% of control levels; Supplemental Figure 3E). ELISA analysis showed that bone marrow serum had 73% lower levels of CXCL14 in 4 month-old *Lepr-cre; Cxcl14*$^{fl/fl}$ mice as compared to littermate

controls but these mice did not differ in terms of CXCL14 levels in blood plasma (Figure 2A). LepR$^+$ cells are thus the major source of CXCL14 in the bone marrow but are not an important source of CXCL14 in the blood.

By flow cytometric analysis, four month-old *Lepr-cre; Cxcl14*$^{fl/fl}$ and littermate control mice did not significantly differ in terms of bone marrow cellularity (Figure 2B) or the frequencies of HSCs (Figure 2C), MPPs (Figure 2D), restricted hematopoietic progenitors (Figure 2E-Q), or differentiated myeloid cells, B cells, T cells, or megakaryocytes (Figure 2R-V) in the bone marrow. They also did not significantly differ in terms of spleen cellularity (Supplemental Figure 3F) or the frequencies of HSCs, MPPs, restricted progenitors, or differentiated hematopoietic cells in the spleen (Supplemental Figure 3G-Y). Finally, *Lepr-cre; Cxcl14*$^{fl/fl}$ and littermate control mice did not significantly differ in the reconstituting potential of bone marrow cells upon competitive transplantation into irradiated mice (Supplemental Figure 3Z) or the frequencies of bone marrow or spleen cells that formed colonies in culture, including megakaryocyte colonies (Supplemental Figure 3AA-AD). CXCL14 is thus not required for HSC maintenance, HSC function, or bone marrow hematopoiesis, including the generation of megakaryocytes.

Four month-old *Lepr-cre; Cxcl14*$^{fl/fl}$ and littermate control mice did not significantly differ in terms of white blood cell (WBC) or red blood cell (RBC) counts but *Lepr-cre; Cxcl14*$^{fl/fl}$ mice had significantly lower platelet counts (Figure 2W; 20% reduction). By 7 months of age, this phenotype was more severe as *Lepr-cre; Cxcl14*$^{fl/fl}$ mice exhibited a 37% reduction in platelet counts, with normal WBC and RBC counts (Figure 2X). Even at 4 months of age, the reduction in platelet counts was associated with prolonged bleeding in *Lepr-cre; Cxcl14*$^{fl/fl}$ as compared to control mice when their tails were severed 1 mm from the end (Figure 2Y).

We would not expect CXCL14 produced by LepR$^+$ in the bone marrow to regulate clotting by platelets in the blood because *Lepr-cre; Cxcl14*$^{fl/fl}$ mice had normal levels of CXCL14 in the blood (Figure 2A) and megakaryocytes and platelets do not express *Cxcl14* (Supplemental Figure 1D-E). Nonetheless, we examined platelet function in these mice and

found that *Lepr-cre; Cxcl14*$^{fl/fl}$ and control mice did not significantly differ in terms of platelet activation (with or without adenosine diphosphate stimulation) or aggregation with leukocytes (Supplemental Figure 4A-D). This is consistent with a prior study that found CXCL14 is not necessary for platelet activation, aggregation, or thrombus formation[47].

Treatment of *Cxcl14*-dsRed mice with anti-CD42b antibody depleted platelets in the blood (Figure 2Z) and significantly increased the numbers of *Cxcl14*-DsRed^{+} stromal cells and LepR^{+}*Cxcl14*-DsRed^{+} stromal cells in the bone marrow (Supplemental Figure 4F and 4G). There was a trend toward increased *Cxcl14* expression by LepR^{+} cells after platelet depletion but the difference was not statistically significant (Supplemental Figure 4H). *LepR-Cre;Cxcl14*$^{fl/fl}$ mice exhibited significantly delayed platelet regeneration, but not white or red blood cell regeneration, as compared to control mice (Figure 2Z). *Cxcl14* expression in the bone marrow thus increased in response to platelet depletion.

LepR-Cre;Cxcl14$^{fl/fl}$ mice also exhibited significantly delayed platelet regeneration, but not white or red blood cell regeneration, as compared to control mice after sublethal irradiation (Figure 2AA). Consistent with the fact that irradiation depletes hematopoietic cells and LepR^{+} cells[61], sublethal irradiation reduced white blood cell, red blood cell, and platelet counts (Figure 2AA) as well as the numbers of *Cxcl14*-DsRed^{+} cells and LepR^{+}*Cxcl14*-DsRed^{+} cells in the bone marrow (Supplemental Figure 4J-M). The level of *Cxcl14*-dsRed expression per LepR^{+} cell also declined after irradiation (Supplemental Figure 4L) consistent with the observation that irradiation broadly reduces hematopoietic growth factor expression by LepR^{+} cells[62].

Cxcl14 **promotes the formation of proplatelet-forming megakaryocytes**

Megakaryocytes grow in size and mature into proplatelet-forming megakaryocytes that extend processes into sinusoidal blood vessels to shed platelets into circulation[22]. Many mature megakaryocytes and proplatelet-forming megakaryocytes are too large and/or too fragile to be observed by flow cytometry[63,64], so we also examined these cells by immunofluorescence

analysis in bone marrow sections (Figure 3A and 3B). *Lepr-cre; Cxcl14*$^{fl/fl}$ and control bone marrow did not significantly differ in terms of the numbers of all CD41^{+} megakaryocytes (Figure 3A-C) but the megakaryocytes in control bone marrow were significantly larger (Figure 3D) and included more proplatelet-forming megakaryocytes (Figure 3E). We did not observe a significant difference in DNA content between CD42d^{+} megakaryocytes from *Lepr-cre; Cxcl14*$^{fl/fl}$ and control mice by flow cytometry (Supplemental Figure 5A-B); however, it is hard to interpret this as the most mature megakaryocytes may have been excluded from this analysis as a result of their size[63,64].

During their maturation, megakaryocytes form a demarcation membrane system that envelops developing platelets in the cytoplasm. By transmission electron microscopy, we observed a significant reduction in demarcation membranes within megakaryocytes from *Lepr-cre; Cxcl14*$^{fl/fl}$ versus control mice (Figure 3F-G), indicating impaired megakaryocyte maturation[65,66].

Arterioles and sinusoids were similar in appearance, density, and diameter in the bone marrow of *Lepr-cre; Cxcl14*$^{fl/fl}$ and control mice (Supplemental Figure 5F-J). CD41^{+} megakaryocytes and proplatelet-forming megakaryocytes were both significantly more likely than all CD45^{+} hematopoietic cells to localize within 10 µm of sinusoids and significantly less likely than all CD45^{+} cells to localize within 10 µm of arterioles (Figure 3H, 3I and Supplemental Figure 5C): 72±7.5% of megakaryocytes and 93±7.4% of proplatelet-forming megakaryocytes were within 10 µm of sinusoids. Moreover, 84±7.8% of megakaryocytes and all proplatelet-forming megakaryocytes were within 10 µm of *Cxcl14*-DsRed^{+} cells (Figure 3J-K). We observed no significant difference in the percentages of megakaryocytes or proplatelet-forming megakaryocytes that localized to sinusoids in *Lepr-cre; Cxcl14*$^{fl/fl}$ versus control mice (Supplemental Figure 5D-E). Lattice light-sheet microscopy revealed that most perisinusoidal megakaryocytes were enveloped by fine processes from *Cxcl14*-DsRed^{+} stromal cells (Figure 3L-M; see also Video 1). Larger megakaryocytes tended to have more interactions (within 1 µm)

per unit surface area with processes from *Cxcl14*-DsRed^{+} cells than smaller megakaryocytes (Supplemental Figure 5K). Megakaryocytes and proplatelet-forming megakaryocytes thus localized mainly to sinusoids but this did not depend upon CXCL14.

To test if CXCL14 functions locally within individual bone marrow compartments or systematically, we assessed hematopoiesis in the long bones (femurs and tibia) and vertebrae of *Prx1-cre; Cxcl14*$^{fl/fl}$ mice and littermate controls. Prx1-cre recombines in limb mesenchyme, including in LepR^{+} cells, but not in vertebrae. We observed no significant differences between *Prx1-cre; Cxcl14*$^{fl/fl}$ and littermate control mice in terms of red or white blood cell counts but *Prx1-cre; Cxcl14*$^{fl/fl}$ mice had significantly lower platelet counts (Supplemental Figure 6A). *Prx1-cre; Cxcl14*$^{fl/fl}$ and littermate control mice also did not significantly differ in body mass, bone marrow cellularity, or the frequencies of hematopoietic stem or progenitor cells by flow cytometry in long bones or vertebrae (Supplemental Figure 6B-AM). However, the number of proplatelet-forming megakaryocytes was significantly lower in femur (Figure 3N), but not vertebra (Figure 3O), bone marrow from *Prx1-cre; Cxcl14*$^{fl/fl}$ mice. This suggests that *Cxcl14* acts locally within individual bone marrow compartments to promote platelet formation.

CXCL14 reprograms lipid metabolism in megakaryocytes

We performed RNA sequencing on megakaryocytes isolated from the bone marrow of *Lepr-cre; Cxcl14*$^{fl/fl}$ and littermate control mice using paramagnetic beads. Four of the ten most significantly enriched Gene Ontology (GO) terms among the differentially expressed genes related to megakaryocyte or platelet differentiation (red highlighted gene sets in Figure 4A). Nearly all of the megakaryocyte and platelet differentiation genes[67] detected by RNA sequencing were significantly downregulated in megakaryocytes from *Lepr-cre; Cxcl14*$^{fl/fl}$ as compared to control mice (red highlighted genes in Figure 4B).

The molecular function GO term most enriched among these genes related to lipid metabolism (Figure 4C). Genes in this GO term were expressed at significantly lower levels in

megakaryocytes from *Lepr-cre; Cxcl14*$^{fl/fl}$ as compared to control mice, including 15 of 17 lipid metabolism genes (Figure 4D). These included *Pparg*, which encodes the PPARγ transcription factor that regulates fatty acid metabolism[68]. PPARγ acts partly by promoting the transcription of fatty acid transporters including *Cd36*, *Fabp5,* and *Fatp4*[69,70]. The levels of PPARγ, FABP5, FATP4 and CD36 protein were all reduced in CD42d^{+} megakaryocytes isolated using paramagnetic beads from the bone marrow of *Lepr-cre; Cxcl14*$^{fl/fl}$ mice (Figure 4E-G). This raised the possibility that megakaryocytes from *Lepr-cre; Cxcl14*$^{fl/fl}$ mice have defects in lipid metabolism, including reduced fatty acid uptake. Changes in lipid metabolism, including increased uptake of polyunsaturated fatty acids, are necessary in megakaryocytes for the formation of proplatelet-forming megakaryocytes and platelets, partly to form the demarcation membrane system[71-74].

To test if PPARγ is necessary for megakaryocyte maturation and platelet formation, we treated wild-type mice with T0070907, a potent and selective inhibitor of PPARγ [75] that can be used to inhibit PPARγ in mice in vivo[76,77]. We confirmed that T0070907 inhibited PPARγ function by treating CD42^{+} megakaryocytes in culture: T0070907 significantly reduced *CD36* and *Fabp4* transcript levels (Supplemental Figure 7A and 7B). Daily intraperitoneal injection of T0070907 for a week did not significantly affect body mass, red or white blood cell counts, bone marrow cellularity, or the frequencies of HSCs, CD41^{+}CD150^{+}LK megakaryocyte progenitors (MkPs), or immature CD41^{+}CD42^{-} megakaryocytes in the bone marrow (Supplemental Figure 7C-H). However, it did significantly reduce platelet counts in the blood (Supplemental Fig. 7D) and the frequencies of more mature CD41^{+}CD42^{+} megakaryocytes in the bone marrow by flow cytometry (Supplemental Figure 7I) as well as the numbers of CD41^{+} megakaryocytes and proplatelet-forming megakaryocytes in bone marrow sections by immunofluorescence analysis (Supplemental Figure 7J and 7K). T0070907 treatment thus phenocopied the depletion of proplatelet-forming megakaryocytes and platelets in *Lepr-cre; Cxcl14*$^{fl/fl}$ mice.

We also treated $CD42^+$ megakaryocytes with recombinant CXCL14 and/or T0070907 in culture. CXCL14 significantly increased the formation of proplatelet-forming megakaryocytes and T0070907 blocked this effect (Supplemental Figure 7L). CXCL14 thus acts directly on megakaryocytes to promote their maturation into proplatelet-forming megakaryocytes in a manner that is mediated by PPARγ.

We performed lipidomic analysis on $CD42d^+$ megakaryocytes isolated using paramagnetic beads from *Lepr-cre; Cxcl14*$^{fl/fl}$ and control bone marrow. We detected 260 lipid species (Supplemental Table 2). All of the lipids that significantly differed between megakaryocytes from *Lepr-cre; Cxcl14*$^{fl/fl}$ and control mice are shown in Figure 4H. Eleven species of triglycerides and 2 species of ceramides were significantly depleted in megakaryocytes from *Lepr-cre; Cxcl14*$^{fl/fl}$ mice. Most of these triglycerides contained polyunsaturated fatty acids, suggesting depletion of polyunsaturated fatty acids in megakaryocytes from *Lepr-cre; Cxcl14*$^{fl/fl}$ mice. While cells can synthesize their own saturated and monounsaturated fatty acids, polyunsaturated fatty acids must be obtained from the diet[78].

To test if CXCL14 from $LepR^+$ cells promotes polyunsaturated fatty acid uptake by megakaryocytes, we infused *Lepr-cre; Cxcl14*$^{fl/fl}$ and littermate control mice for 24 hours with $^{13}C_{18}$-linoleic acid, then isolated $CD42d^+$ megakaryocytes from the bone marrow using paramagnetic beads. We observed no significant difference in the fractional enrichment of $^{13}C_{18}$-linoleic acid ($^{13}C_{18}$-linolaic acid/all linoleic acid) in blood plasma from *Lepr-cre; Cxcl14*$^{fl/fl}$ and control mice (Figure 4I) but *Lepr-cre; Cxcl14*$^{fl/fl}$ megakaryocytes exhibited significantly reduced fractional enrichment as compared to control megakaryocytes (Figure 4J). This suggests that bone marrow megakaryocytes have less capacity to take up polyunsaturated fatty acids from circulation in the absence of CXCL14 from $LepR^+$ cells.

CXCL14 is considered an orphan chemokine, with unknown receptor[52]. Nonetheless, evidence has been presented for several potential receptors including CXCR4[46,47], Low-density lipoprotein receptor-related protein 1 (LRP1[50]), Insulin-like growth factor 1 receptor (IGF1R[48]),

Atypical chemokine receptor 2 (ACKR2[51]), and G protein coupled receptor 85 (GPR85[49]). By RNA sequencing, only *Cxcr4*, *Lrp1*, and *Igf1r* transcripts were detected in bone marrow megakaryocytes (Supplemental Figure 7M). By flow cytometric analysis, we detected CXCR4 on 52±6.5% of CD42d$^+$ megakaryocytes, while LRP1 and IGF1R were present on 47±4.8% and 12±2.2% of CD42d$^+$ megakaryocytes, respectively (Supplemental Figure 7N and 7O). The percentage of CD42d$^+$ megakaryocytes that were positive for these candidate receptors did not significantly differ between *LepR-Cre;Cxcl14$^{fl/fl}$* and control mice (Supplemental Figure 7O). Future studies will be required to assess which candidate receptors mediate the effect of CXCL14 on megakaryocyte maturation.

A high-fat diet rescued platelet formation in *Lepr-cre; Cxcl14$^{fl/fl}$* mice

If the defects in platelet formation were caused by reduced fatty acid uptake, we hypothesized these defects would be rescued by feeding the mice a high fat diet, which would increase the abundance of circulating fatty acids. To test this, we fed *Lepr-cre; Cxcl14$^{fl/fl}$* and littermate control mice normal chow (10% of calories from fat) or either of two high fat diets (both with 60% of calories from fat; Figure 5A). Both high fat diets significantly increased body mass in *Lepr-cre; Cxcl14$^{fl/fl}$* and control mice as compared to mice fed normal chow (Figure 5B). Neither diet nor mouse genotype significantly altered white blood cell counts (Figure 5C), red blood cell counts (Figure 5D), or bone marrow cellularity (Figure 5F). Platelet counts were significantly reduced in the blood of *Lepr-cre; Cxcl14$^{fl/fl}$* as compared to control mice fed normal chow but did not significantly differ between *Lepr-cre; Cxcl14$^{fl/fl}$* and control mice fed either high fat diet (Figure 5E). High fat diets thus rescued platelet production in *Lepr-cre; Cxcl14$^{fl/fl}$* mice.

Lepr-cre; Cxcl14$^{fl/fl}$ and control mice did not exhibit significant differences in the frequencies of any hematopoietic stem or progenitor cell population in the bone marrow by flow cytometry, irrespective of diet (Supplemental Figure 8A-M). Similarly, neither diet nor mouse genotype significantly affected the number of CD41$^+$ megakaryocytes in bone marrow sections

(Figure 5G). The size of these megakaryocytes was significantly reduced in *Lepr-cre; Cxcl14*$^{fl/fl}$ as compared to control mice fed normal chow but no statistically significant difference was observed in mice fed either high fat diet (Figure 5H-I). The number of proplatelet-forming megakaryocytes was significantly reduced in the bone marrow of *Lepr-cre; Cxcl14*$^{fl/fl}$ as compared to control mice fed normal chow but not in mice fed a high fat diet (Figure 5J). A high fat diet did not significantly alter *Cxcl14* expression in the bone marrow or CXCL14 levels in bone marrow or blood (Supplemental Figure 8Q-T).

The triglycerides that were depleted in *Lepr-cre; Cxcl14*$^{fl/fl}$ megakaryocytes from mice fed normal chow (Supplemental Figure 8N) were not depleted in *Lepr-cre; Cxcl14*$^{fl/fl}$ megakaryocytes from mice fed a high fat diet (Supplemental Figure 8O-P; see Supplemental Tables 3-5 for lists of the lipid species detected). A high fat diet thus eliminated the depletion of triglycerides containing polyunsaturated fatty acids in addition to rescuing the formation of proplatelet-forming megakaryocytes and platelets. This suggests that high fat diets acted by increasing the abundance of dietary polyunsaturated fatty acids, which facilitated uptake by megakaryocytes despite lower expression of fatty acid transporters in *Lepr-cre; Cxcl14*$^{fl/fl}$ mice.

Recombinant CXCL14 is sufficient to promote thrombopoiesis

We cultured CD42d^{+} bone marrow cells with or without recombinant CXCL14 (100 ng/ml). CXCL14 significantly increased the numbers of proplatelet-forming megakaryocytes that formed in culture after 16 to 40 hours (Figure 6B). Since only megakaryocytes were present in these cultures, this observation suggests that CXCL14 acts directly on megakaryocytes to promote their maturation into proplatelet-forming megakaryocytes.

We also intravenously injected wild-type mice with 20 µg/kg recombinant mouse CXCL14 and then analyzed the bone marrow 16 hours later. CXCL14-treated and control mice did not significantly differ in terms of white blood cell or red blood cell counts but the CXCL14-treated mice had significantly higher platelet counts (Figure 6C-E). CXCL14-treated and control

mice also did not significantly differ in terms of bone marrow cellularity or the frequencies of HSCs, MPPs, restricted hematopoietic progenitors, or megakaryocytes in the bone marrow by flow cytometry (Figure 6F-T) or in bone marrow sections (Figure 6U-V). However, CXCL14-treated mice had significantly larger megakaryocytes (Figure 6W) and more proplatelet-forming megakaryocytes in the bone marrow as compared to control mice (Figure 6X). Treatment of wild-type mice with CXCL14 was thus sufficient to increase the formation of proplatelet-forming megakaryocytes and platelets.

DISCUSSION

CXCL14 appeared to promote the formation of proplatelet-forming megakaryocytes and platelets by remodeling lipid metabolism in megakaryocytes. Increased polyunsaturated fatty acid uptake is necessary in megakaryocytes to form the demarcation membrane system[71,72]. The triglyceride depletion in the lipidomic analysis of megakaryocytes from *Lepr-cre; Cxcl14*$^{fl/fl}$ mice (Figure 4H) may reflect the consumption of triglycerides in an effort to sustain demarcation membrane synthesis in the absence of CXCL14. A high fat diet rescued the depletion of lipids and the numbers of proplatelet-forming megakaryocytes and platelets in *Lepr-cre; Cxcl14*$^{fl/fl}$ mice (Figure 5E-M). To our knowledge, these data provide the first evidence that LepR^{+} cells regulate metabolism and terminal differentiation in some hematopoietic cells.

The fatty acid transporters whose expression declined in megakaryocytes from *Lepr-cre; Cxcl14*$^{fl/fl}$ mice as compared to littermate controls (CD36, FATP4, and FABP5) are not specific for polyunsaturated fatty acids[79]. Yet polyunsaturated fatty acid-containing lipids were most prominently depleted from these megakaryocytes (Figure 4H). Cells can synthesize their own saturated and monounsaturated fatty acids, but not polyunsaturated fatty acids, potentially compensating for the reduced uptake of saturated and monounsaturated fatty acids[78,80]. It is also possible that the depletion of polyunsaturated fatty acid-containing triglycerides in

megakaryocytes from *Lepr-cre; Cxcl14*$^{fl/fl}$ mice reflects broader defects in lipid uptake or lipid metabolism, not just reduced expression of fatty acid transporters.

ACKNOWLEDGEMENTS

S.J.M. is a Howard Hughes Medical Institute (HHMI) Investigator, the Mary McDermott Cook Chair in Pediatric Genetics, the Kathryn and Gene Bishop Distinguished Chair in Pediatric Research, the director of the Hamon Laboratory for Stem Cells and Cancer, and a Cancer Prevention and Research Institute of Texas Scholar. This study was supported partly by funding from the National Institutes of Health (DK118745 to S.J.M.) and the Moody Medical Research Institute (to S.J.M.). R.J.D. is an HHMI Investigator and is supported by NIH grant R35CA220449. DL is a scholar of Blood Cancer United. TPM and the CRI Metabolomics Facility are supported by funding from the Cancer Prevention Research Institute of Texas (CPRIT Core Facilities Support Award RP240494). We thank the BioHPC high performance computing cloud at UT Southwestern Medical Center for providing computational resources and the Moody Foundation Flow Cytometry Facility. We thank the electron microscopy core facility, supported by NIH grant 1S10OD021685. This article is subject to HHMI's Open Access to Publications policy. HHMI lab heads have previously granted a nonexclusive CC BY 4.0 license to the public and a sublicensable license to HHMI in their research articles. Pursuant to those licenses, the author-accepted manuscript of this article can be made freely available under a CC BY 4.0 license immediately upon publication.

AUTHOR CONTRIBUTIONS

Y.X. and S.J.M. conceived the project and designed and interpreted experiments. Y.X. performed most of the experiments, with general technical assistance from A.R. and R.Z. and advice and technical assistance in the lipidomic analysis experiments from S.M. and G.G.. M.L. performed the western blots and T.T. implanted jugular catheters in mice for isotope-labelled

linoleic acid infusion. T.M., Y.L., W.G., and R.D. helped to perform and analyze the isotope tracing experiments. T.N., Z.S., E.J., and K.D. provided the light-sheet microscopy platform, performed the imaging, and analyzed the light-sheet imaging data. N.J., T.W., and L.D. helped to prepare samples and perform flow cytometry in experiments that involved many mice. Y.Z. and D.L. originally observed the fine processes from LepR$^+$ cells that envelop megakaryocytes and suggested we test if this was true of CXCL14-expressing cells. Z.Z. performed statistical analyses. Y.X. and S.J.M. wrote the manuscript.

CONFLICT OF INTEREST DISCLOSURE

The authors declare no competing interests.

REFERENCES

1. Ding L, Saunders TL, Enikolopov G, Morrison SJ. Endothelial and perivascular cells maintain haematopoietic stem cells. *Nature*. 2012;481(7382):457-462.
2. Comazzetto S, Murphy MM, Berto S, Jeffery E, Zhao Z, Morrison SJ. Restricted Hematopoietic Progenitors and Erythropoiesis Require SCF from Leptin Receptor+ Niche Cells in the Bone Marrow. *Cell Stem Cell*. 2019;24(3):477-486 e476.
3. Oguro H, Ding L, Morrison SJ. SLAM family markers resolve functionally distinct subpopulations of hematopoietic stem cells and multipotent progenitors. *Cell Stem Cell*. 2013;13(1):102-116.
4. Ding L, Morrison SJ. Haematopoietic stem cells and early lymphoid progenitors occupy distinct bone marrow niches. *Nature*. 2013;495(7440):231-235.
5. Greenbaum A, Hsu YM, Day RB, et al. CXCL12 in early mesenchymal progenitors is required for haematopoietic stem-cell maintenance. *Nature*. 2013;495(7440):227-230.
6. Himburg HA, Termini CM, Schlussel L, et al. Distinct Bone Marrow Sources of Pleiotrophin Control Hematopoietic Stem Cell Maintenance and Regeneration. *Cell Stem Cell*. 2018;23(3):370-381 e375.
7. Cordeiro Gomes A, Hara T, Lim VY, et al. Hematopoietic Stem Cell Niches Produce Lineage-Instructive Signals to Control Multipotent Progenitor Differentiation. *Immunity*. 2016;45(6):1219-1231.
8. Emoto T, Lu J, Sivasubramaniyam T, et al. Colony stimulating factor-1 producing endothelial cells and mesenchymal stromal cells maintain monocytes within a perivascular bone marrow niche. *Immunity*. 2022;55(5):862-878 e868.
9. Zhong L, Lu J, Fang J, et al. Csf1 from marrow adipogenic precursors is required for osteoclast formation and hematopoiesis in bone. *Elife*. 2023;12.
10. Inoue K, Qin Y, Xia Y, et al. Bone marrow Adipoq-lineage progenitors are a major cellular source of M-CSF that dominates bone marrow macrophage development, osteoclastogenesis, and bone mass. *Elife*. 2023;12.
11. Omatsu Y, Sugiyama T, Kohara H, et al. The essential functions of adipo-osteogenic progenitors as the hematopoietic stem and progenitor cell niche. *Immunity*. 2010;33(3):387-399.

12. Sugiyama T, Kohara H, Noda M, Nagasawa T. Maintenance of the hematopoietic stem cell pool by CXCL12-CXCR4 chemokine signaling in bone marrow stromal cell niches. *Immunity*. 2006;25(6):977-988.
13. Zhang J, Wu Q, Johnson CB, et al. In situ mapping identifies distinct vascular niches for myelopoiesis. *Nature*. 2021;590(7846):457-462.
14. Wu Q, Zhang J, Kumar S, et al. Resilient anatomy and local plasticity of naive and stress haematopoiesis. *Nature*. 2024;627(8005):839-846.
15. Acar M, Kocherlakota KS, Murphy MM, et al. Deep imaging of bone marrow shows non-dividing stem cells are mainly perisinusoidal. *Nature*. 2015;526(7571):126-130.
16. Shen B, Tasdogan A, Ubellacker JM, et al. A mechanosensitive peri-arteriolar niche for osteogenesis and lymphopoiesis. *Nature*. 2021;591(7850):438-444.
17. Zhou BO, Ding L, Morrison SJ. Hematopoietic stem and progenitor cells regulate the regeneration of their niche by secreting Angiopoietin-1. *Elife*. 2015;4:e05521.
18. Fang S, Chen S, Nurmi H, et al. VEGF-C protects the integrity of the bone marrow perivascular niche in mice. *Blood*. 2020;136(16):1871-1883.
19. Gao X, Murphy MM, Peyer JG, et al. Leptin receptor(+) cells promote bone marrow innervation and regeneration by synthesizing nerve growth factor. *Nat Cell Biol*. 2023;25(12):1746-1757.
20. Gawaz M, Vogel S. Platelets in tissue repair: control of apoptosis and interactions with regenerative cells. *Blood*. 2013;122(15):2550-2554.
21. Asquith NL, Carminita E, Camacho V, et al. The bone marrow is the primary site of thrombopoiesis. *Blood*. 2024;143(3):272-278.
22. Machlus KR, Italiano JE, Jr. The incredible journey: From megakaryocyte development to platelet formation. *J Cell Biol*. 2013;201(6):785-796.
23. Stegner D, vanEeuwijk JMM, Angay O, et al. Thrombopoiesis is spatially regulated by the bone marrow vasculature. *Nat Commun*. 2017;8(1):127.
24. Avecilla ST, Hattori K, Heissig B, et al. Chemokine-mediated interaction of hematopoietic progenitors with the bone marrow vascular niche is required for thrombopoiesis. *Nat Med*. 2004;10(1):64-71.
25. Junt T, Schulze H, Chen Z, et al. Dynamic visualization of thrombopoiesis within bone marrow. *Science*. 2007;317(5845):1767-1770.
26. Kaushansky K, Lok S, Holly RD, et al. Promotion of megakaryocyte progenitor expansion and differentiation by the c-Mpl ligand thrombopoietin. *Nature*. 1994;369(6481):568-571.
27. de Sauvage FJ, Hass PE, Spencer SD, et al. Stimulation of megakaryocytopoiesis and thrombopoiesis by the c-Mpl ligand. *Nature*. 1994;369(6481):533-538.
28. Wendling F, Maraskovsky E, Debili N, et al. cMpl ligand is a humoral regulator of megakaryocytopoiesis. *Nature*. 1994;369(6481):571-574.
29. Debili N, Masse JM, Katz A, Guichard J, Breton-Gorius J, Vainchenker W. Effects of the recombinant hematopoietic growth factors interleukin-3, interleukin-6, stem cell factor, and leukemia inhibitory factor on the megakaryocytic differentiation of CD34+ cells. *Blood*. 1993;82(1):84-95.
30. Briddell RA, Bruno E, Cooper RJ, Brandt JE, Hoffman R. Effect of c-kit ligand on in vitro human megakaryocytopoiesis. *Blood*. 1991;78(11):2854-2859.
31. Avraham H, Vannier E, Cowley S, et al. Effects of the stem cell factor, c-kit ligand, on human megakaryocytic cells. *Blood*. 1992;79(2):365-371.
32. Metcalf D, Hilton D, Nicola NA. Leukemia inhibitory factor can potentiate murine megakaryocyte production in vitro. *Blood*. 1991;77(10):2150-2153.
33. Sakamoto H, Ochiya T, Sato Y, et al. Adenovirus-mediated transfer of the HST-1 (FGF4) gene induces increased levels of platelet count in vivo. *Proc Natl Acad Sci U S A*. 1994;91(26):12368-12372.

34. Konishi H, Ochiya T, Sakamoto H, et al. Effective prevention of thrombocytopenia in mice using adenovirus-mediated transfer of HST-1 (FGF-4) gene. *J Clin Invest*. 1995;96(2):1125-1130.
35. Bruno E, Briddell RA, Cooper RJ, Hoffman R. Effects of recombinant interleukin 11 on human megakaryocyte progenitor cells. *Exp Hematol*. 1991;19(5):378-381.
36. Ishibashi T, Burstein SA. Interleukin 3 promotes the differentiation of isolated single megakaryocytes. *Blood*. 1986;67(5):1512-1514.
37. Ishibashi T, Kimura H, Uchida T, Kariyone S, Friese P, Burstein SA. Human interleukin 6 is a direct promoter of maturation of megakaryocytes in vitro. *Proc Natl Acad Sci U S A*. 1989;86(15):5953-5957.
38. Teramura M, Kobayashi S, Hoshino S, Oshimi K, Mizoguchi H. Interleukin-11 enhances human megakaryocytopoiesis in vitro. *Blood*. 1992;79(2):327-331.
39. Decker M, Leslie J, Liu Q, Ding L. Hepatic thrombopoietin is required for bone marrow hematopoietic stem cell maintenance. *Science*. 2018;360(6384):106-110.
40. Chen S, Hu M, Shen M, et al. IGF-1 facilitates thrombopoiesis primarily through Akt activation. *Blood*. 2018;132(2):210-222.
41. Nishimura S, Nagasaki M, Kunishima S, et al. IL-1alpha induces thrombopoiesis through megakaryocyte rupture in response to acute platelet needs. *J Cell Biol*. 2015;209(3):453-466.
42. Machlus KR, Johnson KE, Kulenthirarajan R, et al. CCL5 derived from platelets increases megakaryocyte proplatelet formation. *Blood*. 2016;127(7):921-926.
43. Gaertner F, Ishikawa-Ankerhold H, Stutte S, et al. Plasmacytoid dendritic cells control homeostasis of megakaryopoiesis. *Nature*. 2024;631(8021):645-653.
44. Hromas R, Broxmeyer HE, Kim C, et al. Cloning of BRAK, a novel divergent CXC chemokine preferentially expressed in normal versus malignant cells. *Biochem Biophys Res Commun*. 1999;255(3):703-706.
45. Dolinska M, Cai H, Mansson A, et al. Characterization of the bone marrow niche in patients with chronic myeloid leukemia identifies CXCL14 as a new therapeutic option. *Blood*. 2023;142(1):73-89.
46. Tanegashima K, Suzuki K, Nakayama Y, et al. CXCL14 is a natural inhibitor of the CXCL12-CXCR4 signaling axis. *FEBS Lett*. 2013;587(12):1731-1735.
47. Witte A, Rohlfing AK, Dannenmann B, et al. The chemokine CXCL14 mediates platelet function and migration via direct interaction with CXCR4. *Cardiovasc Res*. 2021;117(3):903-917.
48. Cheng CL, Yang SC, Lai CY, et al. CXCL14 Maintains hESC Self-Renewal through Binding to IGF-1R and Activation of the IGF-1R Pathway. *Cells*. 2020;9(7).
49. Wang Y, Weng X, Wang L, et al. HIC1 deletion promotes breast cancer progression by activating tumor cell/fibroblast crosstalk. *J Clin Invest*. 2018;128(12):5235-5250.
50. Miyajima R, Tanegashima K, Naruse N, Denda M, Hara T, Otaka A. Identification of Low-Density Lipoprotein Receptor-Related Protein 1 as a CXCL14 Receptor Using Chemically Synthesized Tetrafunctional Probes. *ACS Chem Biol*. 2024;19(2):551-562.
51. Zhang Q, Zhou N, Wang W, Zhou S. A Novel Autocrine CXCL14/ACKR2 Axis: The Achilles' Heel of Cancer Metastasis? *Clin Cancer Res*. 2019;25(12):3476-3478.
52. Al Hamwi G, Namasivayam V, Buschbell B, Gedschold R, Golz S, Muller CE. Proinflammatory chemokine CXCL14 activates MAS-related G protein-coupled receptor MRGPRX2 and its putative mouse ortholog MRGPRB2. *Commun Biol*. 2024;7(1):52.
53. Salogni L, Musso T, Bosisio D, et al. Activin A induces dendritic cell migration through the polarized release of CXC chemokine ligands 12 and 14. *Blood*. 2009;113(23):5848-5856.
54. Lu J, Chatterjee M, Schmid H, Beck S, Gawaz M. CXCL14 as an emerging immune and inflammatory modulator. *J Inflamm (Lond)*. 2016;13:1.
55. DeFalco J, Tomishima M, Liu H, et al. Virus-assisted mapping of neural inputs to a feeding center in the hypothalamus. *Science*. 2001;291(5513):2608-2613.

56. Logan M, Martin JF, Nagy A, Lobe C, Olson EN, Tabin CJ. Expression of Cre Recombinase in the developing mouse limb bud driven by a Prxl enhancer. *Genesis*. 2002;33(2):77-80.
57. Wang X, Menezes CJ, Jia Y, et al. Metabolic inflexibility promotes mitochondrial health during liver regeneration. *Science*. 2024;384(6701):eadj4301.
58. Faubert B, Tasdogan A, Morrison SJ, Mathews TP, DeBerardinis RJ. Stable isotope tracing to assess tumor metabolism in vivo. *Nat Protoc*. 2021;16(11):5123-5145.
59. Kara N, Xue Y, Zhao Z, et al. Endothelial and Leptin Receptor(+) cells promote the maintenance of stem cells and hematopoiesis in early postnatal murine bone marrow. *Dev Cell*. 2023;58(5):348-360 e346.
60. Du LM, Freitas MA, Zhang JZ, et al. Periarteriolar niches become inflamed in aging bone marrow, remodeling the stromal microenvironment and depleting lymphoid progenitors. *Proceedings of the National Academy of Sciences of the United States of America*. 2025;122(11).
61. Zhou BO, Yu H, Yue R, et al. Bone marrow adipocytes promote the regeneration of stem cells and haematopoiesis by secreting SCF. *Nat Cell Biol*. 2017;19(8):891-903.
62. Mo C, Guo J, Qin J, et al. Single-cell transcriptomics of LepR-positive skeletal cells reveals heterogeneous stress-dependent stem and progenitor pools. *EMBO J*. 2022;41(4):e108415.
63. McGrath KE. Utilization of imaging flow cytometry to define intermediates of megakaryopoiesis in vivo and in vitro. *J Immunol Methods*. 2015;423:45-51.
64. Pedersen MN, Hybel TE, Bjerre JH, et al. High-Efficiency Enrichment of Megakaryocytes and Identification of Micromegakaryocytes from Human Bone Marrow by Imaging Flow Cytometry. *Cells*. 2025;14(8).
65. Mazzi S, Lordier L, Debili N, Raslova H, Vainchenker W. Megakaryocyte and polyploidization. *Exp Hematol*. 2018;57:1-13.
66. Eckly A, Heijnen H, Pertuy F, et al. Biogenesis of the demarcation membrane system (DMS) in megakaryocytes. *Blood*. 2014;123(6):921-930.
67. Haas S, Hansson J, Klimmeck D, et al. Inflammation-Induced Emergency Megakaryopoiesis Driven by Hematopoietic Stem Cell-like Megakaryocyte Progenitors. *Cell Stem Cell*. 2015;17(4):422-434.
68. Ahmadian M, Suh JM, Hah N, et al. PPARgamma signaling and metabolism: the good, the bad and the future. *Nat Med*. 2013;19(5):557-566.
69. Goto K, Iso T, Hanaoka H, et al. Peroxisome proliferator-activated receptor-gamma in capillary endothelia promotes fatty acid uptake by heart during long-term fasting. *J Am Heart Assoc*. 2013;2(1):e004861.
70. Tontonoz P, Nagy L, Alvarez JGA, Thomazy VA, Evans RM. PPARγ promotes monocyte/macrophage differentiation and uptake of oxidized LDL. *Cell*. 1998;93(2):241-252.
71. de Jonckheere B, Kollotzek F, Munzer P, et al. Critical shifts in lipid metabolism promote megakaryocyte differentiation and proplatelet formation. *Nat Cardiovasc Res*. 2023;2:835-852.
72. Barrachina MN, Pernes G, Becker IC, et al. Efficient megakaryopoiesis and platelet production require phospholipid remodeling and PUFA uptake through CD36. *Nat Cardiovasc Res*. 2023;2(8):746-763.
73. Siddiqui NF, Shabrani NC, Kale VP, Limaye LS. Enhanced generation of megakaryocytes from umbilical cord blood-derived CD34(+) cells expanded in the presence of two nutraceuticals, docosahexanoic acid and arachidonic acid, as supplements to the cytokine-containing medium. *Cytotherapy*. 2011;13(1):114-128.
74. Dhenge A, Limbkar K, Melinkeri S, Kale VP, Limaye L. Arachidonic acid and Docosahexanoic acid enhance platelet formation from human apheresis-derived CD34(+) cells. *Cell Cycle*. 2017;16(10):979-990.

75. Lee G, Elwood F, McNally J, et al. T0070907, a selective ligand for peroxisome proliferator-activated receptor gamma, functions as an antagonist of biochemical and cellular activities. *J Biol Chem*. 2002;277(22):19649-19657.
76. Guo YB, Zhu YC, Sun Y, Yang HX. The preventive effect of low-dose aspirin in a PPAR-γ antagonist treated mouse model of preeclampsia. *Bmc Pregnancy and Childbirth*. 2022;22(1).
77. Wei M, Guo M, Meng X, et al. PPARgamma Mediates the Cardioprotective Roles of Danlou Tablet After Acute Myocardial Ischemia-Reperfusion Injury. *Front Cardiovasc Med*. 2022;9:858909.
78. Jeon YG, Kim YY, Lee G, Kim JB. Physiological and pathological roles of lipogenesis. *Nat Metab*. 2023;5(5):735-759.
79. Stahl A, Gimeno RE, Tartaglia LA, Lodish HF. Fatty acid transport proteins: a current view of a growing family. *Trends Endocrinol Metab*. 2001;12(6):266-273.
80. Rohrig F, Schulze A. The multifaceted roles of fatty acid synthesis in cancer. *Nat Rev Cancer*. 2016;16(11):732-749.

FIGURE LEGENDS

Figure 1: LepR$^+$ stromal cells were the main source of *Cxcl14* in the bone marrow.

(A) Single cell RNA sequencing[59] showing *Cxcl14* expression by LepR$^+$ stromal cells from enzymatically dissociated bone and bone marrow (a total of 3-4 mice from 3 independent experiments). (B) *Cxcl14* expression by quantitative reverse-transcription PCR in CD150$^+$CD48$^-$ Lineage$^-$Sca1$^+$ckit$^+$ HSCs, CD31$^+$CD45$^-$Ter119$^-$ endothelial cells, LepR$^+$CD45$^-$Ter119$^-$CD31$^-$ stromal cells, and unfractionated cells from the bone marrow of two month-old mice (a total of 3 samples per cell population from 3 independent experiments; each dot represents a different sample). (C and D) Deep confocal imaging of femur bone marrow from adult *Cxcl14*^{dsRed}*Scf*^{GFP} mice: *Cxcl14*-dsRed$^+$ cells localized around sinusoids (arrowheads) and arterioles (arrow) throughout bone marrow (white dashed lines indicate the interface of bone marrow and bone; see also the low magnification image of a whole bone in Supplemental Figure 1C). Most *Cxcl14*-dsRed$^+$ cells were *Scf*-GFP$^+$ (images are representative of 3 mice). (E) Femur bone marrow from adult *Cxcl14*^{dsRed} mice stained with anti-LepR antibody showing that most *Cxcl14*-dsRed$^+$ cells were LepR$^+$ (images are representative of 3 mice). (F-J) Flow cytometric analysis of enzymatically dissociated bone marrow from *Cxcl14*$^{dsRed/+}$ or *Cxcl14*^{dsRed}*Scf*^{GFP} mice. Only 0.19±0.04% of bone marrow cells from *Cxcl14*$^{dsRed/+}$ mice were *Cxcl14*-dsRed$^+$ and, of these, 91% were LepR$^+$ (F). Conversely, 89% of LepR$^+$ cells were *Cxcl14*-dsRed$^+$ (G). 84% of LepR$^+$ cells from bone marrow of *Cxcl14*^{dsRed}*Scf*^{GFP} mice were *Cxcl14*-dsRed$^+$ and *Scf*-GFP$^+$ (H). Few CD31$^+$CD45$^-$Ter119$^-$ endothelial cells from bone marrow of *Cxcl14*$^{dsRed/+}$ mice were *Cxcl14*-dsRed$^+$ (I; 3-6 mice from 3 independent experiments). (J) Flow cytometric analysis of non-enzymatically dissociated bone marrow shows few or no CD45$^+$ cells expressed *Cxcl14*-dsRed (3-6 mice from 3 independent experiments; see also Supplemental Figure1D). Data represent mean ± standard deviation in panels B, F, G, and I.

Figure 2: *Lepr-cre; Cxcl14$^{fl/fl}$* mice exhibited grossly normal hematopoiesis but reduced platelet counts. (A) ELISA of CXCL14 levels in bone marrow serum and blood plasma from *Lepr-cre; Cxcl14$^{fl/fl}$* and control mice (a total 4 mice per group from 2 independent experiments). (B-V) Bone marrow cellularity (B) and the frequencies of HSCs (C), MPPs (D), HPCs (E), CMPs (F), GMPs (G), MEPs (H), CLPs (I), Pre-GMs (J), Pre-CFUEs (K), CFU-Es (L), Pre-MegEs (M), megakaryocyte progenitors (N), Pre-proB cells (O), ProB cells (P), PreB cells (Q), Mac1^{+}Gr1^{+} myeloid cells (R), B220^{+}IgM^{+} B cells (S), CD3^{+} T cells (T), CD41^{+}CD42d^{-} megakaryocytes (U) and CD41^{+}CD42d^{+} megakaryocytes (V) in the bone marrow of *Lepr-cre; Cxcl14 $^{fl/fl}$* and littermate control mice (a total of 4-17 mice per genotype from 3-7 independent experiments). (W) White blood cell (WBC), red blood cell (RBC) and platelet (PLT) counts in the blood of *Lepr-cre; Cxcl14$^{fl/fl}$* mice and littermate controls at 4 months of age (W; a total of 16-17 mice per genotype from 7 independent experiments) and 7 months of age (X; a total of 4-5 mice per genotype from 3 independent experiments). (Y) Bleeding time after severing the tail 1 mm from the end in *Lepr-cre; Cxcl14$^{fl/fl}$* and control mice (a total of 14-15 mice per genotype from 3 independent experiments). (Z) WBC, RBC and PLT counts from the blood of *Lepr-cre; Cxcl14$^{fl/fl}$* and control mice before (day 0) and 2, 4, 6 and 12 days after treatment with anti-CD42b antibody to deplete platelets (a total of 6 mice per genotype from 2 independent experiments). (AA) WBC, RBC and PLT counts from *Lepr-cre; Cxcl14$^{fl/fl}$* and control mice before (day 0) and 7, 14, 28 and 35 days after sublethal irradiation (a total of 4-8 mice per genotype from 2 independent experiments). All data represent mean ± standard deviation and each dot represents a different mouse in panels A-Y. All statistical tests were two-sided. Statistical significance was assessed using a matched samples two-way ANOVA followed by Sidak's multiple comparisons adjustment (A), Student's *t*-tests (B and Y), Mann-Whitney tests followed by Holm-Sidak's multiple comparisons adjustments (C-V), or Student's *t*-tests followed by Holm-Sidak's multiple comparisons adjustments (W, X, Z and AA).

Figure 3: *Lepr-cre; Cxcl14$^{fl/fl}$* mice produced fewer proplatelet-forming megakaryocytes in the bone marrow. (A) Representative images of femur bone marrow from adult *Lepr-cre; Cxcl14$^{fl/fl}$* and control mice showing CD41^{+} proplatelet-forming megakaryocytes (arrows; images are representative of 3 independent experiments). (B) High magnification image of a CD41^{+} proplatelet-forming megakaryocyte adjacent to a sinusoid. (C) The number of CD41^{+} megakaryocytes per mm^{2} in bone marrow sections did not significantly differ between *Lepr-cre; Cxcl14$^{fl/fl}$* and control mice (3 mice per genotype from 3 independent experiments). (D) Distribution of CD41^{+} megakaryocyte cell diameters (3 mice per genotype from 3 independent experiments). (E) The number of CD41^{+} proplatelet-forming megakaryocytes (PPF MKs) per mm^{2} in bone marrow sections (3 mice per genotype from 3 independent experiments). (F, G) Transmission microscopy images of megakaryocytes in the bone marrow of *Lepr-cre; Cxcl14$^{fl/fl}$* and control mice showed reduced demarcation membrane system (DMS) in megakaryocytes from mutant mice (3 mice per genotype from 3 independent experiments; each dot represents a megakaryocyte). (H, I) CD41^{+} megakaryocytes (H) and CD41^{+} proplatelet-forming megakaryocytes (I) were significantly more likely than all CD45^{+} cells to localize adjacent to sinusoids and less likely to localize adjacent to arterioles (a total of 3 mice per group from 3 independent experiments). (J, K) CD41^{+} megakaryocytes (J) and CD41^{+} proplatelet-forming megakaryocytes (K) were significantly more likely than all CD45^{+} cells to localize adjacent to *Cxcl14*-dsRed^{+} stromal cells (3 or 5 mice per group from 3 independent experiments). (L, M) Representative images of femur bone marrow from *Cxcl14^{dsRed}* mice showing fine processes from *Cxcl14^{+}* stromal cells wrapping around CD41^{+} megakaryocytes (images are representative of 4 independent experiments). (N, O) The number of CD41^{+} proplatelet-forming megakaryocytes (PPF MKs) per mm^{2} of bone marrow sections from femurs (N) or vertebrae (O) of *Prx1-cre; Cxcl14$^{fl/fl}$* and control mice (6 or 9 mice per genotype from 3 or 4 independent experiments). All data represent mean ± standard deviation and each dot represents a different

mouse except in panels D and G. All statistical tests were two-sided. Statistical significance was assessed using matched samples two-way ANOVAs followed by Sidak's multiple comparisons adjustments (C and E), nested *t*-tests (D and G), Student's *t*-tests (H, I, J, K, and N), or Mann-Whitney tests (K and O) followed by Holm-Sidak's multiple comparisons adjustments.

Figure 4: Megakaryocytes from *Lepr-cre; Cxcl14$^{fl/fl}$* mice exhibited changes in lipid metabolism as compared to control megakaryocytes. (A-D) We performed RNA sequencing on megakaryocytes from the bone marrow of *Lepr-cre; Cxcl14$^{fl/fl}$* and control mice (3 mice per genotype from 3 independent experiments). (A) The 10 most significant Gene Ontology (GO) terms that were enriched for genes differentially expressed among *Lepr-cre; Cxcl14$^{fl/fl}$* and control megakaryocytes (log2 fold change > 0.5 in either direction and FDR < 0.05), including GO terms related to biological processes (BP), cellular components (CC) and molecular function (MF). GO terms highlighted in red contain genes involved in megakaryocyte and platelet differentiation or function. (B) Heatmap of genes involved in megakaryocyte or platelet differentiation (z scores; list of genes is from ref[67]). (C) The 10 most significantly enriched GO terms related to molecular function (MF) from genes that were differentially expressed among *Lepr-cre; Cxcl14$^{fl/fl}$* and control megakaryocytes (log2 fold change >0.5 in either direction and FDR < 0.05). (D) Heatmap of genes from the lipid binding GO term that were directly related to lipid metabolism (z scores). (E-G) Western blot of proteins that regulate lipid metabolism or fatty acid transport in extracts from CD42d^{+} megakaryocytes isolated using paramagnetic beads from *Lepr-cre; Cxcl14$^{fl/fl}$* or littermate control bone marrow (results are representative of 2 samples per genotype from 2 independent experiments). (H) Lipidomic analysis of CD42d^{+} megakaryocytes from *Lepr-cre; Cxcl14$^{fl/fl}$* and control bone marrow. Significantly changed lipid species (FDR<0.05, log2 FC>0.5 in either direction) in megakaryocytes from *Lepr-cre; Cxcl14$^{fl/fl}$* as compared to control bone marrow. (I and J) Fractional enrichment of $^{13}C_{18}$-linoleic acid in

blood plasma or megakaryocytes from *Lepr-cre; Cxcl14*$^{fl/fl}$ and control mice after intravenous infusion of $^{13}C_{18}$-linoleic acid for 24 hours (a total of 7 mice per genotype from 2 independent experiments). All statistical tests were two-sided. Statistical significance was assessed using the Omics Data Analyzer (see lipidomics methods; H), a Mann-Whitney test (I) and a Student's *t*-test (J) followed by Holm-Sidak's multiple comparisons adjustments.

Figure 5: High-fat diet feeding rescued thrombopoiesis in *Lepr-cre; Cxcl14*$^{fl/fl}$ mice. (A-M) *Lepr-cre; Cxcl14*$^{fl/fl}$ and littermate control mice were fed normal chow (10% of calories from fat) or either of two high fat diets (HFD1 and HFD2, both of which had 60% of calories from fat) for four weeks. (B) Body mass of *Lepr-cre; Cxcl14*$^{fl/fl}$ and control mice after 4 weeks on these diets (a total of 3-13 mice per genotype per diet from 2-3 independent experiments). (C-F) Blood cell counts and bone marrow cellularity (F) in *Lepr-cre; Cxcl14*$^{fl/fl}$ and control mice fed each diet (a total of 3-16 mice per genotype per diet from 2-3 independent experiments; each dot represents a different mouse). (G-I) The number of CD41^{+} megakaryocytes per mm^{2} in sections through the bone marrow (G) and the cell diameter distribution of these cells in mice fed normal chow versus HFD1 (H) or normal chow versus HFD2 (I). (J) The number of CD41^{+} proplatelet-forming megakaryocytes per mm^{2} in sections through the bone marrow of mice on control, HFD1, or HFD2 diets (3 mice per genotype from 3 independent experiments in G-J). All data represent mean ± standard deviation and each dot represents a different mouse except in panels H and I. All statistical tests were two-sided. Statistical significance was assessed using two-way ANOVAs followed by Sidak's or Dunnett's multiple comparisons adjustments (B, F, G, and J), Mann-Whitney tests followed by Holm-Sidak's multiple comparisons adjustments (C-E), a nested one-way ANOVAs followed by Sidak's multiple comparisons adjustments (H and I).

Figure 6: Recombinant CXCL14 is sufficient to increase the production of proplatelet-forming megakaryocytes and platelets. (A, B) Proplatelet-forming megakaryocytes (arrows)

formed by CD42^{-} bone marrow cells cultured with or without 100 ng/mL recombinant mouse CXCL14 (rmCXCL14) (images are representative of 5 independent experiments). (C-X) Wild-type mice were intravenously injected with recombinant mouse CXCL14 and then analyzed 16 hours later. Panels C-T show 6 mice per treatment from 3 independent experiments. (C-E) Blood cell counts. (F-T) Bone marrow cellularity (F) and the frequencies of HSCs (G), MPPs (H), HPCs (I), CLPs (J), CMPs (K), GMPs (L), MEPs (M), Pre-GMs (N), Pre-CFU-Es (O), CFU-Es (P), Pre-MegEs (Q), megakaryocyte progenitors (R), CD41^{+}CD42d^{-} megakaryocytes (S) and CD41^{+}CD42d^{+} megakaryocytes (T) in the bone marrow. (U) CD41^{+} megakaryocytes in femur diaphysis bone marrow (arrows point to proplatelet-forming megakaryocytes; images are representative of 4 mice per treatment from 3 independent experiments). (V and W) Number of CD41^{+} megakaryocytes per mm^{2} in diaphysis bone marrow sections (V) as well as cell diameter distribution (W) (4 mice per group from 3 independent experiments). (X) Number of CD41^{+} proplatelet-forming megakaryocytes per mm^{2} in diaphysis bone marrow sections (4 mice per treatment from 3 independent experiments). (Y) Schematic summary. All data represent mean ± standard deviation and each dot represents a different mouse except in panels B and W. All statistical tests were two-sided. Statistical significance was assessed using Student's *t*-tests followed by Holm-Sidak's multiple comparisons adjustments (C-E), a Student's *t*-test (F), matched samples two-way ANOVAs followed by Sidak's multiple comparisons adjustments (B, G-T, V, and X), or a nested *t*-test (W).

Figure 1

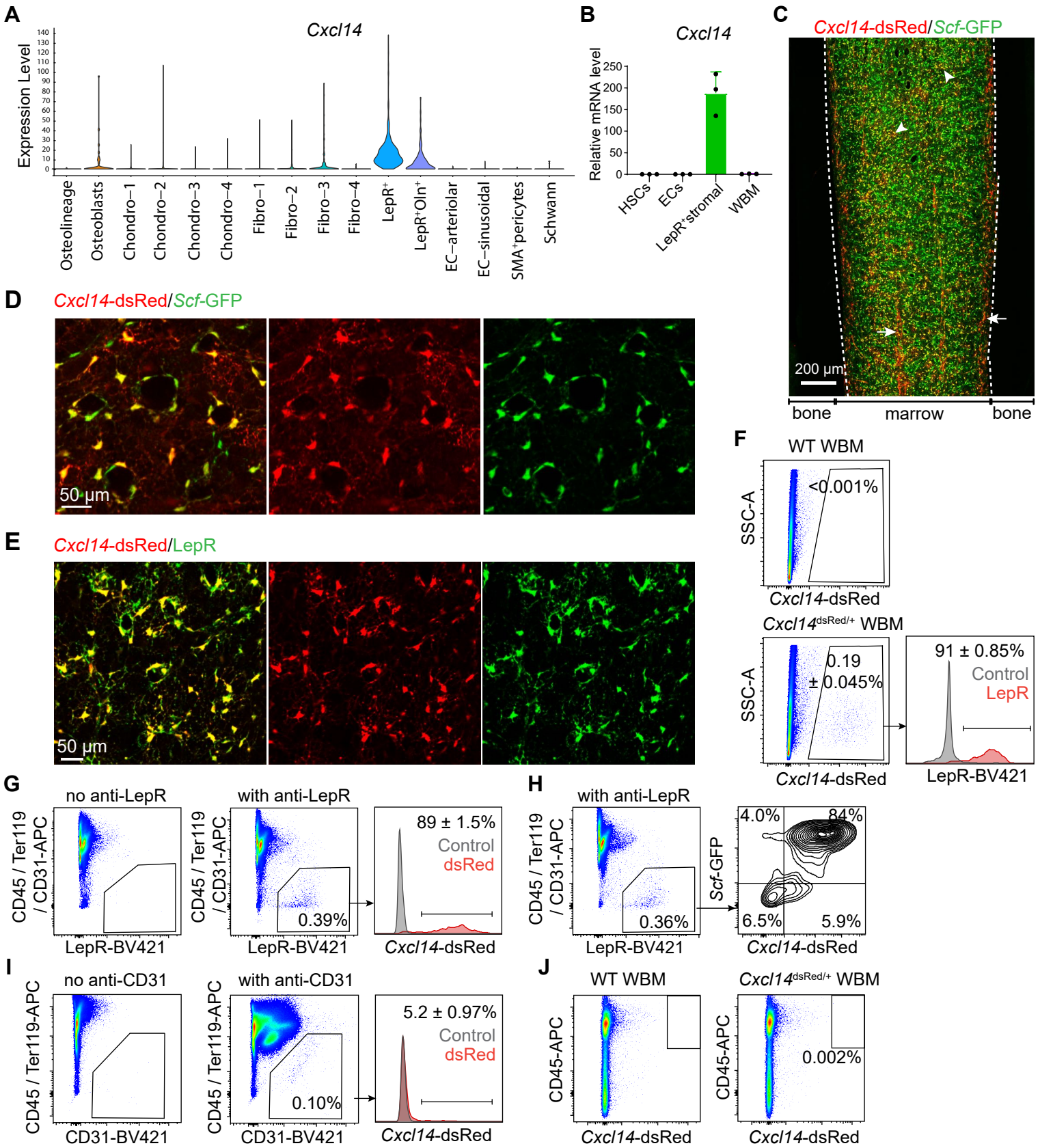
A
Cxcl14
Expression Level
Osteolineage
Osteoblasts
Chondro−1
Chondro−2
Chondro−3
Chondro−4
Fibro−1
Fibro−2
Fibro−3
Fibro−4
LepR+
LepR+Oln+
EC−arteriolar
EC−sinusoidal
SMA+pericytes
Schwann
B
Cxcl14
Relative mRNA level
HSCs
ECs
LepR+stromal
WBM
C
Cxcl14-dsRed/Scf-GFP
200 µm
bone
marrow
bone
D
Cxcl14-dsRed/Scf-GFP
50 µm
E
Cxcl14-dsRed/LepR
50 µm
F
WT WBM
<0.001%
SSC-A
Cxcl14-dsRed
Cxcl14dsRed/+ WBM
0.19
± 0.045%
91 ± 0.85%
Control
LepR
LepR-BV421
G
no anti-LepR
with anti-LepR
CD45 / Ter119 / CD31-APC
LepR-BV421
0.39%
89 ± 1.5%
Control
dsRed
Cxcl14-dsRed
H
with anti-LepR
0.36%
Scf-GFP
4.0%
84%
6.5%
5.9%
I
no anti-CD31
with anti-CD31
CD45 / Ter119-APC
CD31-BV421
0.10%
5.2 ± 0.97%
Control
dsRed
Cxcl14-dsRed
J
WT WBM
Cxcl14dsRed/+ WBM
CD45-APC
0.002%

Figure 2

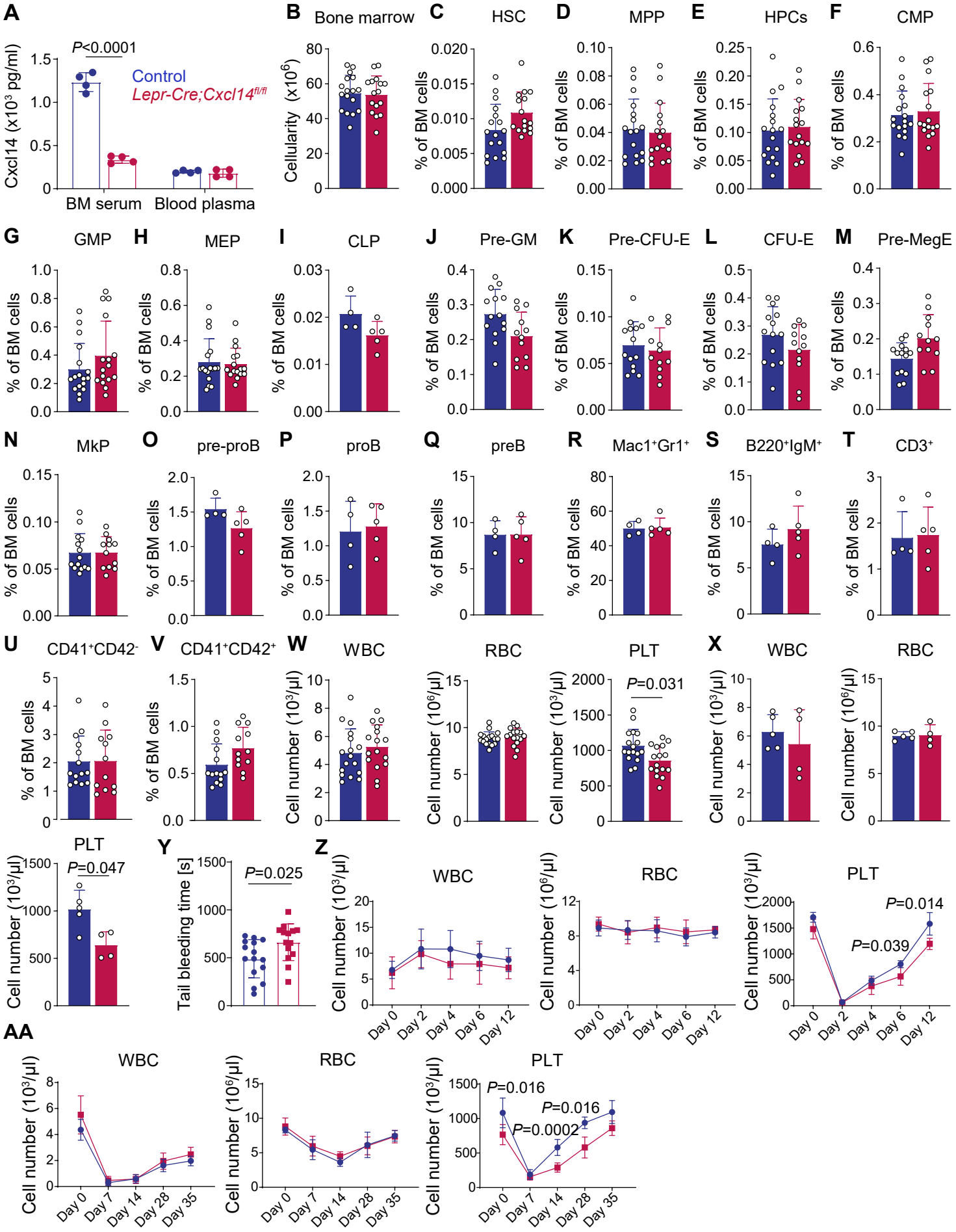
A
P<0.0001
Control
Lepr-Cre;Cxcl14fl/fl
Cxcl14 (x10³ pg/ml)
BM serum
Blood plasma
B Bone marrow
Cellularity (x10⁶)
C HSC
D MPP
E HPCs
F CMP
% of BM cells
G GMP
H MEP
I CLP
J Pre-GM
K Pre-CFU-E
L CFU-E
M Pre-MegE
N MkP
O pre-proB
P proB
Q preB
R Mac1⁺Gr1⁺
S B220⁺IgM⁺
T CD3⁺
U CD41⁺CD42⁻
V CD41⁺CD42⁺
W WBC
RBC
PLT
P=0.031
X WBC
RBC
PLT
P=0.047
Y
Tail bleeding time [s]
P=0.025
Z
WBC
RBC
PLT
P=0.014
P=0.039
Cell number (10³/μl)
Cell number (10⁶/μl)
Day 0
Day 2
Day 4
Day 6
Day 12
AA
WBC
RBC
PLT
P=0.016
P=0.016
P=0.0002
Day 0
Day 7
Day 14
Day 28
Day 35

Figure 3

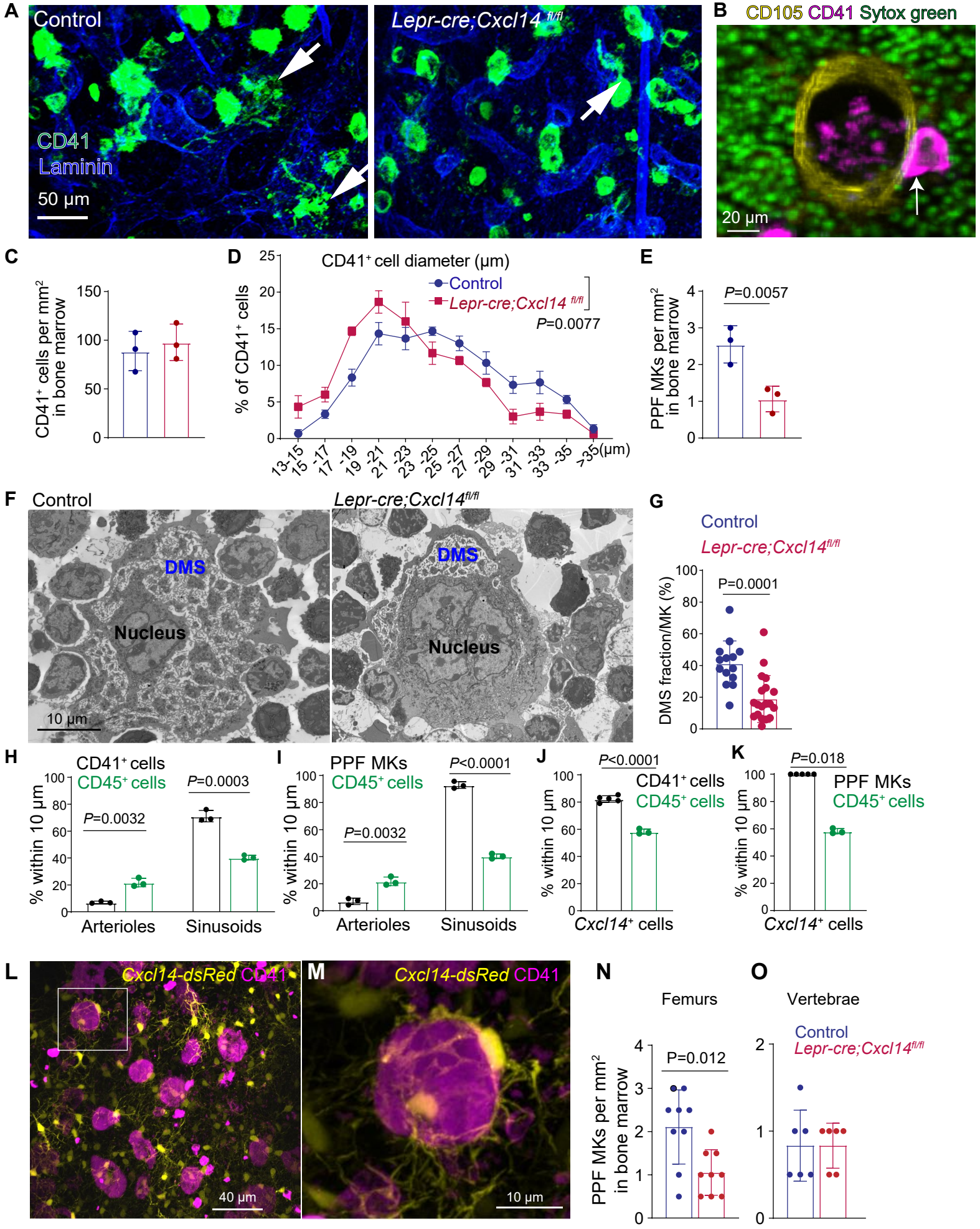
A
Control
Lepr-cre;Cxcl14 fl/fl
CD41
Laminin
50 μm
B
CD105 CD41 Sytox green
20 μm
C
CD41+ cells per mm2 in bone marrow
D
CD41+ cell diameter (μm)
Control
Lepr-cre;Cxcl14 fl/fl
P=0.0077
% of CD41+ cells
13-15
15-17
17-19
19-21
21-23
23-25
25-27
27-29
29-31
31-33
33-35
>35(μm)
E
P=0.0057
PPF MKs per mm2 in bone marrow
F
Control
Lepr-cre;Cxcl14fl/fl
DMS
Nucleus
10 μm
G
Control
Lepr-cre;Cxcl14fl/fl
P=0.0001
DMS fraction/MK (%)
H
CD41+ cells
CD45+ cells
P=0.0032
P=0.0003
% within 10 μm
Arterioles
Sinusoids
I
PPF MKs
CD45+ cells
P=0.0032
P<0.0001
% within 10 μm
Arterioles
Sinusoids
J
P<0.0001
CD41+ cells
CD45+ cells
% within 10 μm
Cxcl14+ cells
K
P=0.018
PPF MKs
CD45+ cells
% within 10 μm
Cxcl14+ cells
L
Cxcl14-dsRed CD41
40 μm
M
Cxcl14-dsRed CD41
10 μm
N
Femurs
P=0.012
PPF MKs per mm2 in bone marrow
O
Vertebrae
Control
Lepr-cre;Cxcl14fl/fl

Figure 4

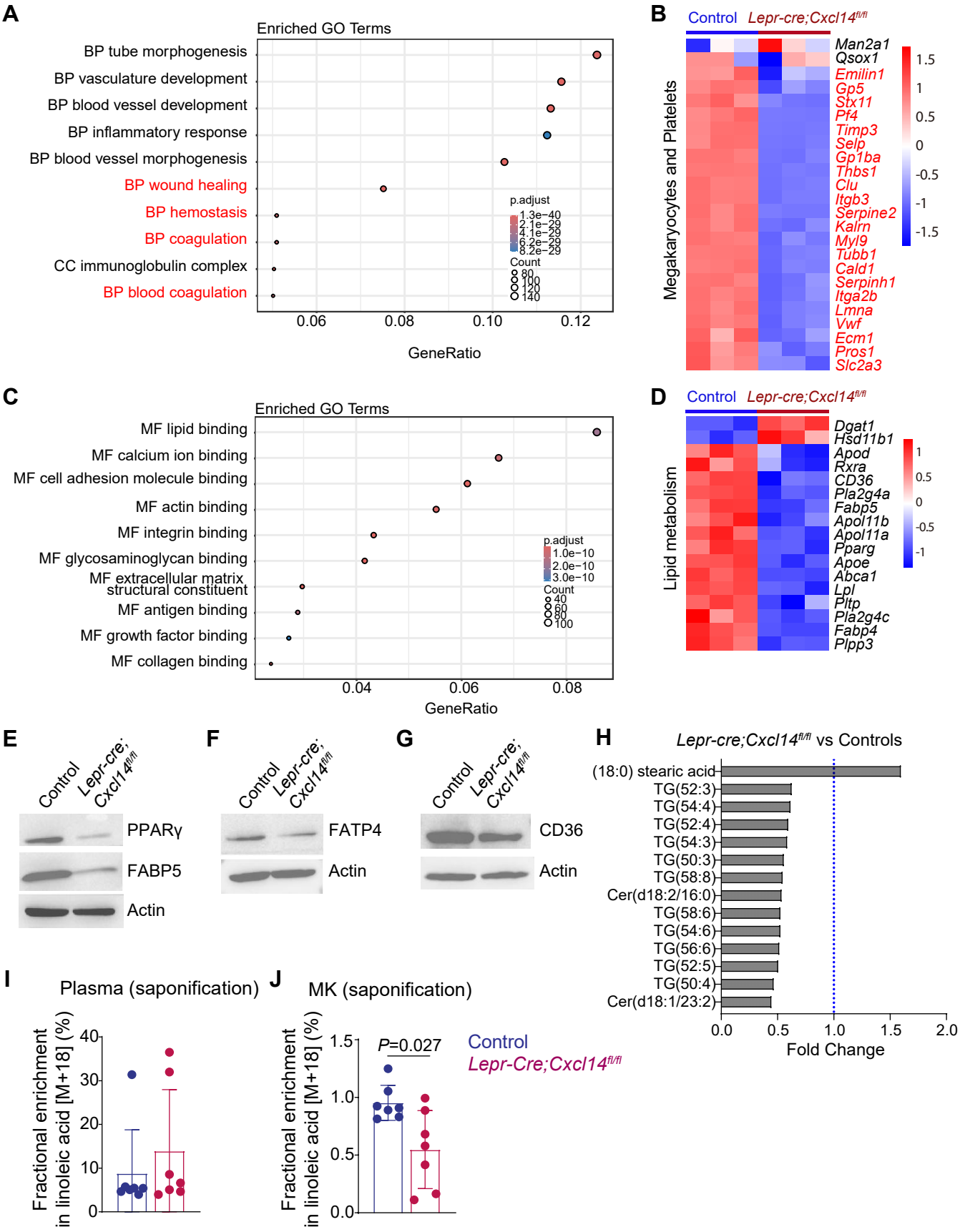
A
Enriched GO Terms
BP tube morphogenesis
BP vasculature development
BP blood vessel development
BP inflammatory response
BP blood vessel morphogenesis
BP wound healing
BP hemostasis
BP coagulation
CC immunoglobulin complex
BP blood coagulation
p.adjust
1.3e−40
2.1e−29
4.1e−29
6.2e−29
8.2e−29
Count
80
100
120
140
0.06
0.08
0.10
0.12
GeneRatio
B
Control
Lepr-cre;Cxcl14fl/fl
Megakaryocytes and Platelets
Man2a1
Qsox1
Emilin1
Gp5
Stx11
Pf4
Timp3
Selp
Gp1ba
Thbs1
Clu
Itgb3
Serpine2
Kalrn
Myl9
Tubb1
Cald1
Serpinh1
Itga2b
Lmna
Vwf
Ecm1
Pros1
Slc2a3
1.5
1
0.5
0
-0.5
-1
-1.5
C
Enriched GO Terms
MF lipid binding
MF calcium ion binding
MF cell adhesion molecule binding
MF actin binding
MF integrin binding
MF glycosaminoglycan binding
MF extracellular matrix structural constituent
MF antigen binding
MF growth factor binding
MF collagen binding
p.adjust
1.0e−10
2.0e−10
3.0e−10
Count
40
60
80
100
0.04
0.06
0.08
GeneRatio
D
Control
Lepr-cre;Cxcl14fl/fl
Lipid metabolism
Dgat1
Hsd11b1
Apod
Rxra
CD36
Pla2g4a
Fabp5
Apol11b
Apol11a
Pparg
Apoe
Abca1
Lpl
Pltp
Pla2g4c
Fabp4
Plpp3
1
0.5
0
-0.5
-1
E
Control
Lepr-cre; Cxcl14fl/fl
PPARγ
FABP5
Actin
F
Control
Lepr-cre; Cxcl14fl/fl
FATP4
Actin
G
Control
Lepr-cre; Cxcl14fl/fl
CD36
Actin
H
Lepr-cre;Cxcl14fl/fl vs Controls
(18:0) stearic acid
TG(52:3)
TG(54:4)
TG(52:4)
TG(54:3)
TG(50:3)
TG(58:8)
Cer(d18:2/16:0)
TG(58:6)
TG(54:6)
TG(56:6)
TG(52:5)
TG(50:4)
Cer(d18:1/23:2)
0.0
0.5
1.0
1.5
2.0
Fold Change
I
Plasma (saponification)
Fractional enrichment in linoleic acid [M+18] (%)
40
30
20
10
0
J
MK (saponification)
Fractional enrichment in linoleic acid [M+18] (%)
P=0.027
1.5
1.0
0.5
0.0
Control
Lepr-Cre;Cxcl14fl/fl

Figure 5

A

Diet	Carbohyrate (kcal%)	Fat (kcal%)	%SFA	%MUFA	%PUFA
Normal	70	10	24	30	47
HFD1	20	60	24	26	50
HFD2	20	60	32	36	32

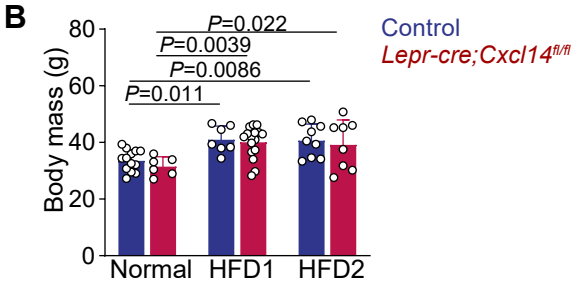

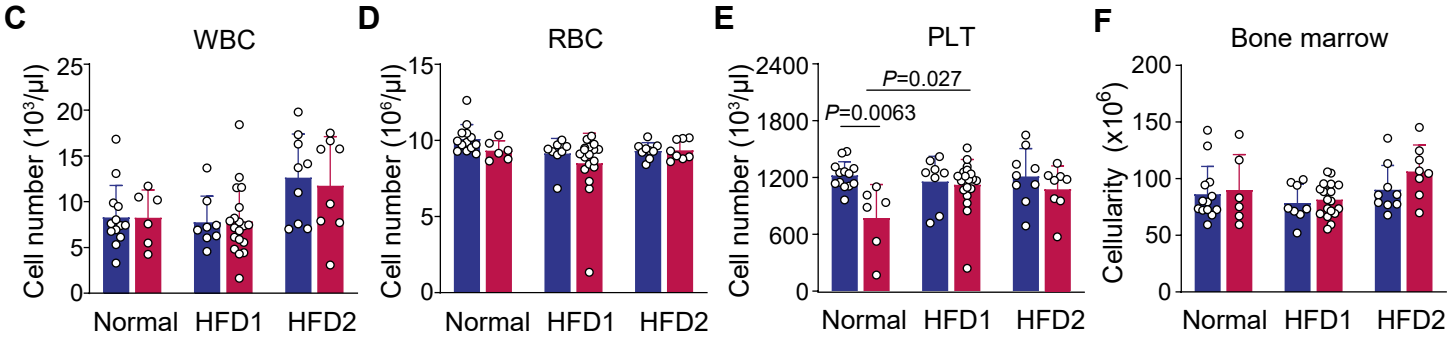

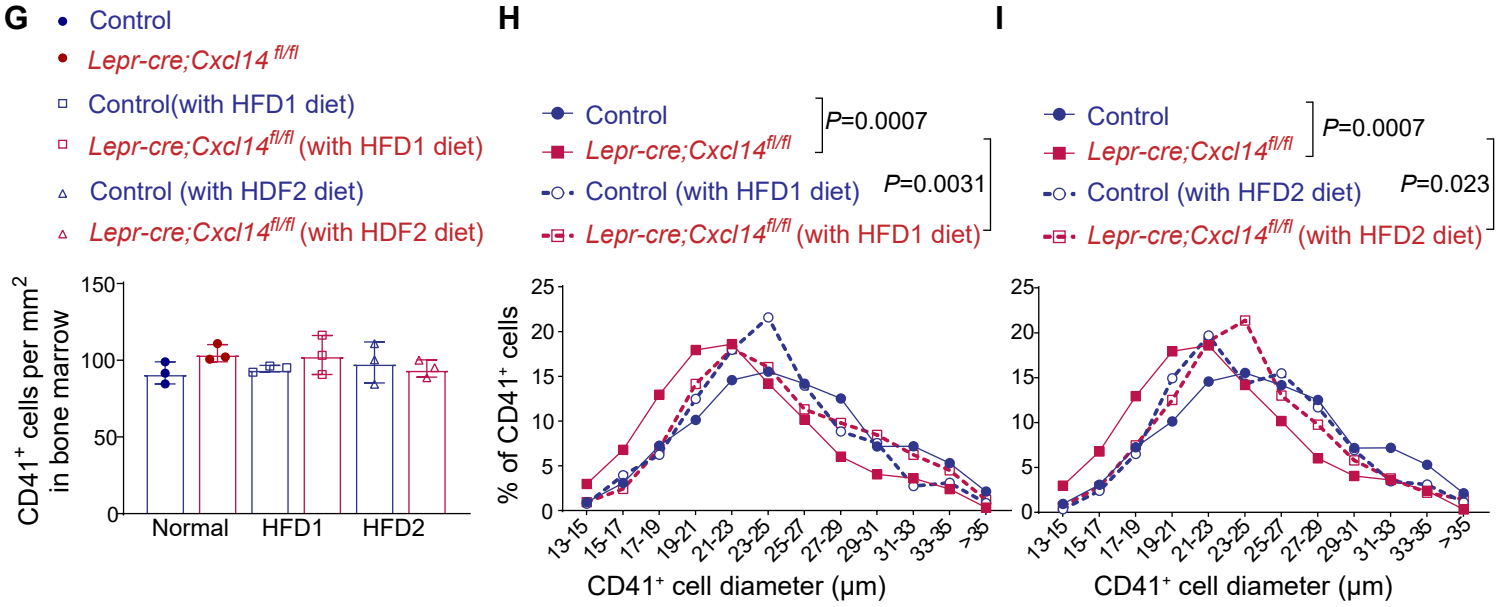

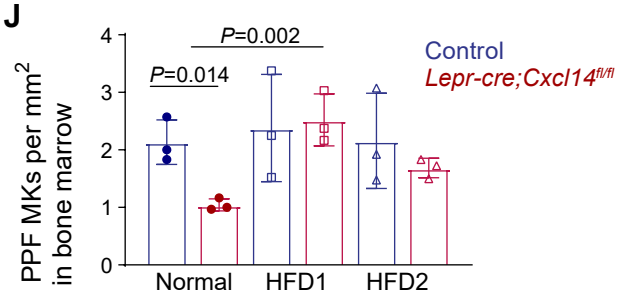

Figure 6

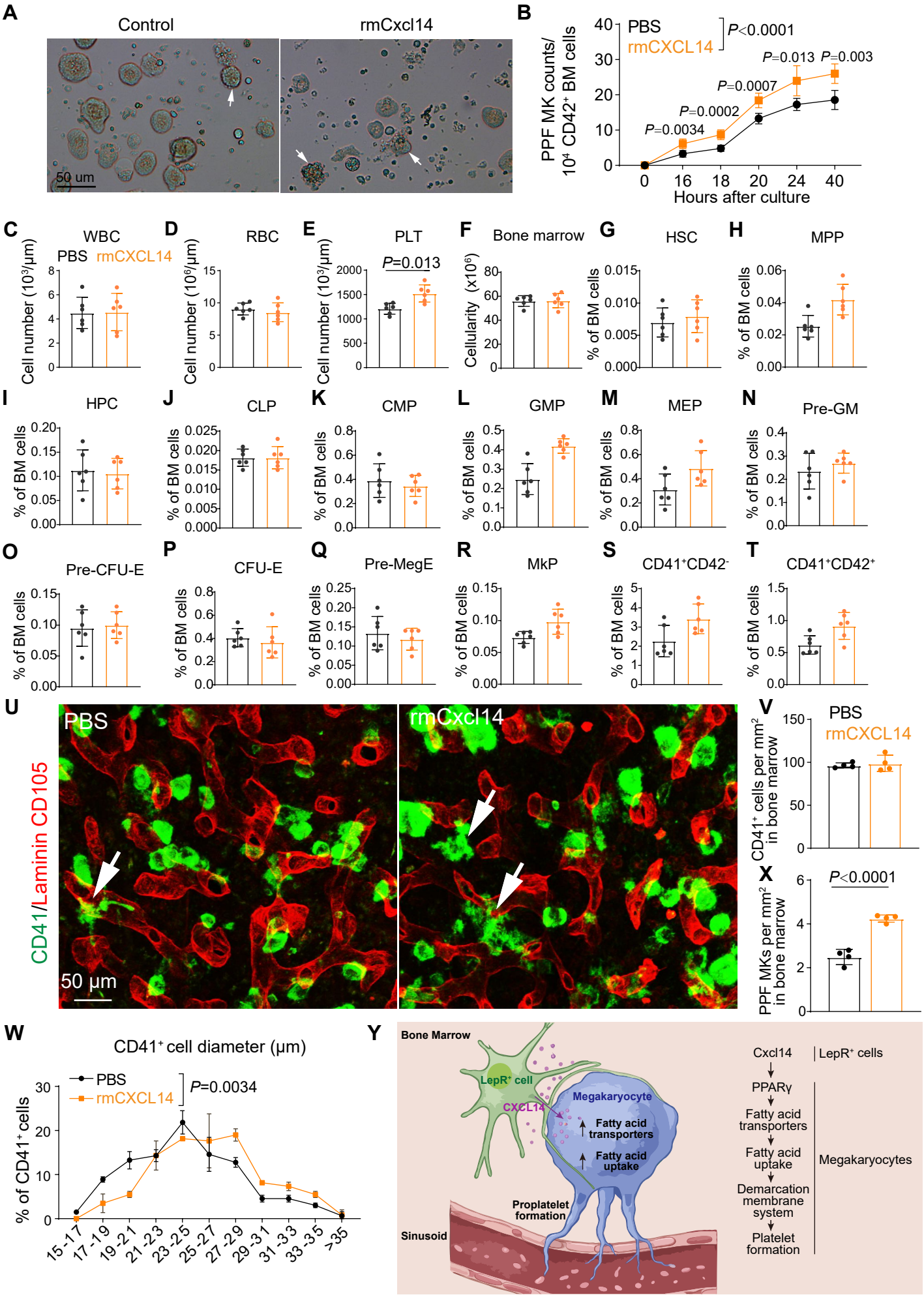
A
Control
rmCxcl14
50 um
B
PPF MK counts/ 10⁴ CD42⁺ BM cells
PBS
rmCXCL14
P<0.0001
P=0.013
P=0.003
P=0.0007
P=0.0002
P=0.0034
Hours after culture
C WBC
D RBC
E PLT
P=0.013
F Bone marrow
G HSC
H MPP
I HPC
J CLP
K CMP
L GMP
M MEP
N Pre-GM
O Pre-CFU-E
P CFU-E
Q Pre-MegE
R MkP
S CD41⁺CD42⁻
T CD41⁺CD42⁺
Cell number (10³/μm)
Cell number (10⁶/μm)
Cellularity (x10⁶)
% of BM cells
U
PBS
rmCxcl14
CD41/Laminin CD105
50 μm
V
CD41⁺ cells per mm² in bone marrow
X
P<0.0001
PPF MKs per mm² in bone marrow
W
CD41⁺ cell diameter (μm)
PBS
rmCXCL14
P=0.0034
% of CD41⁺ cells
15-17
17-19
19-21
21-23
23-25
25-27
27-29
29-31
31-33
33-35
>35
Y
Bone Marrow
LepR⁺ cell
CXCL14
Megakaryocyte
Fatty acid transporters
Fatty acid uptake
Proplatelet formation
Sinusoid
Cxcl14
LepR⁺ cells
PPARγ
Fatty acid transporters
Fatty acid uptake
Demarcation membrane system
Platelet formation
Megakaryocytes